PACS numbers: 61.16.Ch, **68.35.–p**, **78.50.–w**
DOI: 10.1070/PU2000v043n05ABEH000756

Tunneling spectroscopy of the localized states of individual impurity atoms on a semiconductor surface

N S Maslova, V I Panov, S V Savinov

Impurity states and atomic defects play a crucial role in the formation of electron systems on semiconductor surfaces and interfaces.

As the size of a system is decreased and its dimensionality reduced, the effect of isolated localized states becomes decisive and makes necessary a comprehensive investigation of their interaction with the surface structure of the crystal [1]. Scanning tunneling microscopy and spectroscopy (STM/STS) [2] is, in our opinion, the most suitable method for such investigations, since it allows one to study the properties of individual localized states and their interactions on a surface and provides the possibility of identifying an isolated impurity atom from STM images and characteristic features in tunneling-conductivity spectra. At the same time, the peculiarities of tunneling in STM contacts, whose dimensions are comparable to interatomic distances, lead to essentially nonequilibrium processes, which results in effects distorting the initial (nonperturbed) density of states and makes the interpretation of experimental data more difficult. The basis of these effects was studied in Refs [3–9] and is consistently taken into account in analyzing experiments.

This paper presents the results of investigations of the isolated localized and interacting impurity states of individual atoms on the surface of III–V semiconductors. Measurements were conducted on the pure (110) surface of GaAs and InAs single crystals with different dopants at a temperature of 4 K.

Figure 1 shows, as a typical example, the STM image of Si and Zn impurity atoms on the (100) surface of GaAs, which differ in the structure and in the localization radius of the impurity state. The salient features of these impurity atoms are determined from the characteristic features in tunneling-conductivity spectra. Figure 2 shows the STM images and STS spectra of Te, Si and Zn impurities on the surface of GaAs. The donor impurity states, Te and Si, have a localization radius of about 4 nm. The acceptor impurity, Zn, has an extended shape determined by the symmetry of the localized orbital, and the localization radius is on the order of 2 nm.

The tunneling-conductivity spectra obtained exhibit some common features. On the plots of tunneling spectra for all impurities and a pure semiconductor surface, the forbidden energy gap is shifted and its width differs from that characteristic of the volume samples. This effect is connected with a band bending induced by a charge occurring at the localized state of an impurity and/or at the tip of an STM because of the finite relaxation time of tunneling electrons. In the curves of tunneling conductivity measured over impurities (regardless of the sign of their charge) there exist peaks in the forbidden gap and at its edges. Such behavior of tunneling conductivity is determined by the Coulomb interaction of localized states, which modifies the initial arrangement of impurity state levels relative to the forbidden-gap edges. The local density of states in the vicinity of an impurity atom

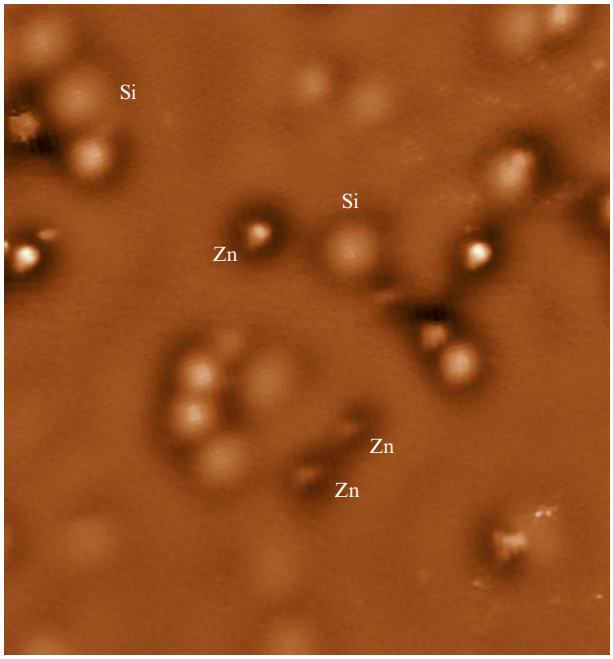

Figure 1. STM image of a portion of the GaAs(110) surface doubly doped with Si and Zn atoms. Image size 40.8×40.8 nm, tunneling voltage $V_t = 1.5$ V.

changes significantly deep in the valence band as well. In particular, for donor impurities Te and Si a decrease in the density of states at energies of about 2 eV is observed, and for an acceptor impurity Zn the density of states in the valence band increases. At the same time each of the impurities studied has well-reproducible individual peculiarities in its tunneling-conductivity spectra.

The interaction of impurity states was studied for two close atoms of Si. The technique developed enabled us for the first time to trace the evolution of the spatial structure of electron density in the vicinity of impurity atoms depending on the potential and determine its connection with the symmetry of the localized states of interacting electrons with a given energy. The sequence of images given in Fig. 3 shows the energy dependence of the regions of mutual overlapping of electron density (obtained shot by shot), which determines the moments the interaction is turned on and off and the symmetry of these states. The degree of overlapping depends on an applied voltage and, hence, can be controlled by an external electric field.

A typical energy range over which the local electron density distribution undergoes considerable changes is on the order of 0.1 eV. This value is comparable with the broadening of the energy levels of localized states resulting from interparticle interactions.

The effect of an additional perturbation potential associated with impurity atoms in the undersurface layer or with the influence of the tip of an STM can lead to the occurrence of an asymmetry in the electron-density distribution in the neighborhood of two interacting impurities up to the extent of forming an electron state localized mainly near one of these impurity atoms.

Peaks in the tunneling conductivity spectra defining the type and interaction of impurity atoms disappear when the distance from a defect reaches a value determined by the maximum of the localization radius for the electron states

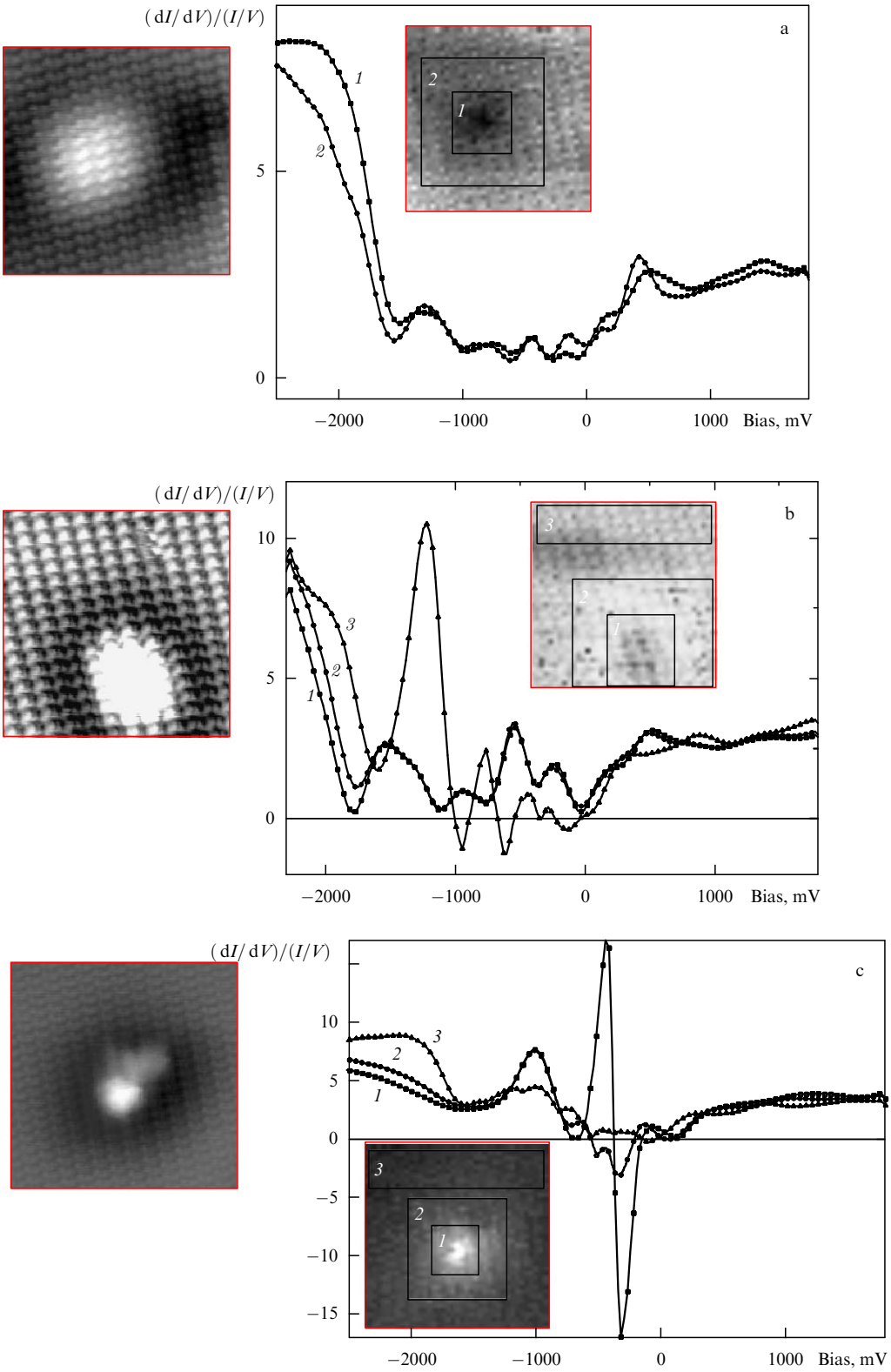

Figure 2. (a) STM image of the impurity state of a Si atom. Image size 5.8×5.8 nm, tunneling voltage $V_t = 1.5$ V. Tunneling conductivity in the vicinity of an Si atom on the GaAs(110) surface. (b) STM image of the impurity state of a Te atom. Image size 5.8×5.8 nm, tunneling voltage $V_t = 1.5$ V. Tunneling conductivity in the vicinity of a Te atom on the GaAs(110) surface. (c) STM image of the impurity state of a Zn atom. Image size 5.8×5.8 nm, tunneling voltage $V_t = 1.5$ V. Tunneling conductivity in the vicinity of a Zn atom on the GaAs(110) surface. In the insets: surface regions for which the plots of tunneling conductivity are presented.

of interacting atoms (for shallow-level impurities it may exceed 10 nm). With distance from a defect, not only the amplitude but also the energy of a peak changes. This is due to the strong dependence of the energy spectrum on the

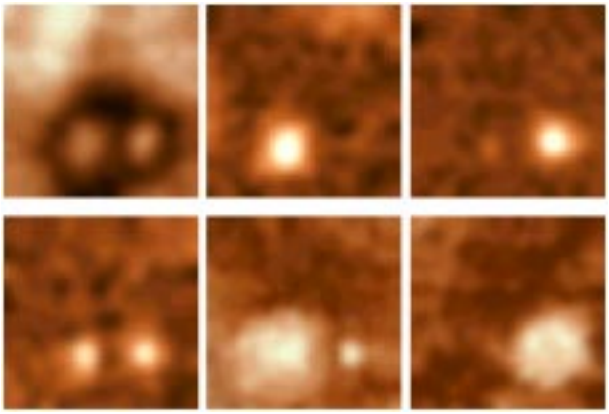

Figure 3. Evolution of the spatial distribution of the local electron density of interacting impurity Si atoms versus energy (tunneling potential applied to a sample). Image size 10×10 nm, $I_t = 400$ pA. Tunneling voltage ranges from -1.5 V to $+1$ V.

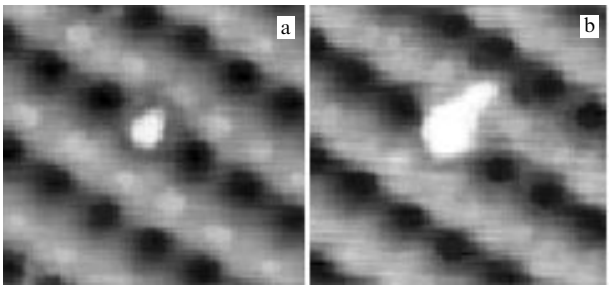

Figure 4. STM image of the space localization of the hybrid orbital of the broken bond of an impurity Cr atom versus tunneling voltage V_t: (a) $V_t = 1$ V, (b) $V_t = 1.1$ V.

Coulomb interaction of electrons localized on impurity atoms.

A theoretical analysis of the energy spectrum and the symmetry of states within the two-site extended Hubbard's model provides a qualitative explanation for the peculiarities of local tunneling-current spectra obtained in experiments.

The technique developed has made possible the detailed study of the formation of the spatial and energy structures of an isolated broken bond on a surface. Figure 4 shows the tunneling-potential dependence of the spatial localization of the broken bond of an impurity atom Cr arising from substitution for As in the InAs lattice. It is seen that the perturbation potential contributed by a transition-metal impurity atom is confined to one crystal lattice period. The region of increased electron density and its shape correspond to the spatial localization of an unpaired electron on the hybrid orbital of the broken bond of Cr with the absent (upper) In atom. The extended shape of the electron cloud and its dependence on the tunneling potential show spatial directionality characteristic of a hybrid orbital with the involvement of a d-electron state. An estimate of the characteristic energy of Coulomb repulsion for the electrons of such a state gives a value $U \sim e^2/a_0 \sim 0.5$ eV (at $a_0 \sim 0.5$ nm) that is comparable to the energy-gap width, which results in the shifting of energy levels observed for STS spectra in the vicinity of deep impurity states.

Based on analysis of the results of STM/STS investigations of different impurity atoms, we have shown the most common features of their tunneling spectra and STM/STS images and have studied the basic effects responsible for the changes in these features, which makes it possible to identify an individual atomic impurity in a semiconductor.

It should also be noted that the method for recording the evolution of the spatial distribution of the local electron density has shown for the first time the possibility of controlling and measuring the states of information bits created on the basis of individual interacting atoms in a semiconductor matrix.

References

1. Madelung O *Festkörpertheorie III. Lokalisierte Zustände* (Berlin: Springer-Verlag, 1973) [Translated into English: *Introduction to Solid-State Theory* (Berlin: Springer-Verlag, 1978)] [Translated into Russian (Moscow: Mir, 1985)]
2. Binnig G, Roher H, Gerber C, Weibel E *Phys. Rev. Lett.* **50** 120 (1983)
3. Maslova N S et al. *Pis'ma Zh. Eksp. Teor. Fiz.* **67** 130 (1998) [*JETP Lett.* **67** 146 (1998)]
4. Maslova N S et al. *Zh. Eksp. Teor. Fiz.* **102** 925 (1992) [*Sov. Phys. JETP* **75** 505 (1992)]
5. Arseev P I, Maslova N S *Zh. Eksp. Teor. Fiz.* **102** 1056 (1992) [*Sov. Phys. JETP* **75** 575 (1992)]
6. Maslova N S, Panov V I *Usp. Fiz. Nauk* **157** 185 (1989) [*Sov. Phys. Usp.* **32** 93 (1989)]
7. Depuydt A et al. *Appl. Phys. A* **66** 171 (1998)
8. Depuydt A et al. *Phys. Rev. B* **60** 2619 (1999)
9. Maslova N S et al. *Phys. Low-Dim. Struct.* (5/6) 131 (1997)
10. Kane B E *Nature* (London) **393** 133 (1998)